Characterization of reciprocity gaps from interference tests in fractured media through a dual porosity model

X. Sanchez-Vila, P. Ackerer, F. Delay, A. Guadagnini

AGU PUBLICATIONS

Water Resources Research

RESEARCH ARTICLE

10.1002/2015WR018171

Key Points:
- Reciprocity gaps of drawdowns can arise in interference tests in fractured media
- Reciprocity gaps emerge mathematically depending on the way the pumping well is embedded in the model
- Nonreciprocity informs on dynamics of fracture/matrix contribution to pumping rates

Correspondence to:
X. Sanchez-Vila,
xavier.sanchez-vila@upc.edu

Citation:
Sanchez-Vila, X., P. Ackerer, F. Delay, and A. Guadagnini (2016), Characterization of reciprocity gaps from interference tests in fractured media through a dual porosity model, *Water Resour. Res.*, *52*, 1696–1704, doi:10.1002/2015WR018171.

Received 29 SEP 2015
Accepted 6 FEB 2016
Accepted article online 11 FEB 2016
Published online 6 MAR 2016

Characterization of reciprocity gaps from interference tests in fractured media through a dual porosity model

X. Sanchez-Vila[1], P. Ackerer[2], F. Delay[2], and A. Guadagnini[3,4]

[1]Hydrogeology Group, Department of Civil and Environmental Engineering, Barcelona, Spain, [2]Laboratoire d'Hydrologie et de Géochimie de Strasbourg, University Strasbourg/EOST, CNRS UMR 7517, Strasbourg, France, [3]Dipartimento di Ingegneria Civile e Ambientale, Politecnico di Milano, Milano, Italy, [4]Department of Hydrology and Water Resources, University of Arizona, Tucson, Arizona, USA

Abstract We analyze drawdown reciprocity gaps emerging in interference tests performed in a confined fissured karstic formation. Modeling the system as a dual porosity continuum allows characterizing the dynamics of the relative contribution of the connected fractures and the rock matrix to the total flow rate extracted at the pumping wells. Observed lack of reciprocity of drawdowns can then be linked to the occurrence of processes that are not accounted for in the classical flow models based on a single-continuum representation of the system through flow equations grounded on Darcy's law only. We show that interpreting the system as a dual porosity continuum can cause drawdown reciprocity gaps to emerge as a consequence of local effects associated with an identifiable contribution of the matrix to the total fluid extracted at the well location during pumping. These theoretical results are then employed to identify the contribution to the flow being supplied to the pumping well by the low conductivity matrix constituting the host rock formation, in contrast to that provided by the fractures. An application to data from two interference tests performed at the Hydrogeological Experimental Site (HES) in Poitiers, France, illustrates the approach. We show that, whenever the matrix is assumed to provide a contribution to the total flow rate extracted, nonreciprocity is expected, the latter being linked to the occurrence of a differential drawdown between fracture and matrix at the pumping well. This difference decreases with time in the example presented, displaying a power law late time behavior, with nonreciprocity effects persisting up to remarkably long times.

1. Introduction

Conceptual models employed to describe fluid flow in fractured reservoirs include (1) explicit representations of discrete fractures embedded in a rock matrix, (2) the adoption of a single equivalent porous continuum, and (3) the use of multiple continua formulations. Reviews of these and other approaches are included in the works of, e.g., *Berkowitz* [2002], *Neuman* [2005], *Sahimi* [2011], and *Ghasemizadeh et al.* [2012]. Among these approaches, we are here concerned with conceptual models based on the depiction of the fractured medium as a system composed by two overlapped continua, according to which a highly conductive medium (representing the collection of fractures in the domain) is embedded within a low conductivity matrix, constituting the host rock. In this context, one can distinguish between dual porosity or dual permeability modeling schemes, depending on whether the host porous rock acts solely as a storage for (or release of) the fluid or also constitutes an active domain for flow. Applications of such models for the analysis and interpretation of fluid flow in natural settings include, among others, the works of *Huyakorn et al.* [1983], *Dershowitz and Miller* [1995], *Huang et al.* [2004], *Samardzioska and Popov* [2005], *Maréchal et al.* [2008], *Bailly et al.* [2009], and *Trottier et al.* [2014]. Analytical solutions for the interpretation of constant-rate pumping tests in fractured systems have also been developed, relying upon the dual porosity approach associated with pseudo steady state exchange between fractures and matrix [*De Smedt*, 2011, and references therein].

An interesting feature of dual continua approaches which we investigate in this work is their ability of giving rise to reciprocity gaps when used in the context of numerical modeling of cross-hole pumping tests. In this context, the drawdown evolution as a function of time observed at a location *A* and induced by pumping at a location *B* is said to be reciprocal with that observed in *B* and due to pumping in *A* when these coincide after normalization by the respective flow rates [e.g., *Bruggeman*, 1972; *Raghavan*, 2009, and references therein].

Recent studies have analyzed the conditions under which drawdown reciprocity gaps during interference tests can be observed. *Mao et al*. [2013] showed by numerical simulations that reciprocity might not hold for flow in variably saturated media. *Delay et al*. [2012] focused on unconfined aquifer systems and found that reciprocity gaps in vertically averaged drawdowns can be related to the occurrence of (*a*) vertical trends in hydraulic conductivity and/or specific storage, or (*b*) significant drainage from the unsaturated zone. *Delay et al*. [2011] stated that reciprocity of modeled drawdowns is inherently linked to the nature of groundwater flow models in fully saturated media based on Darcian concepts applied to porous or fractured, homogeneous or heterogeneous systems, provided they are represented as a single equivalent continuum.

Delay et al. [2011] further analyzed the possibility of emergence of reciprocity gaps in the context of dual continua representations of fractured reservoirs. They demonstrated rigorously that, in these settings and under general transient conditions, reciprocity holds only for drawdowns that occur within the fractures. Otherwise, modeled drawdowns in the matrix continuum are generally nonreciprocal. The analytical developments of *Delay et al*. [2011] are based on treating the pumping wells as sink/source terms operating in the fracture continuum.

Here we address the following objectives: (a) to assess the implications on modeled reciprocity gaps of treating the pumping well as a model boundary to the governing dual porosity formulation, and (b) to provide an approach to characterize the way the rock matrix contributes to the global flow rate extracted at the pumping well. We consider these questions by analyzing through a dual porosity model reciprocity gaps observed during standard interference tests in a fractured rock formation. The motivation underlying the study of the first problem is related to the observation that pumping rates are considered as boundary terms in convergent flow scenarios (see, e.g., *De Smedt* [2011] for a dual porosity setting), while being typically included in standard numerical models of groundwater flows by modeling wells as source/sink terms. It is then relevant to provide an appropriate characterization of the effects that the mathematical representation of an external stress such as pumping can exert on the pressure and flow distributions governed by the model we analyze.

A key driver to our study of the second objective is the observation that, while the rock matrix is typically considered to provide only a negligible contribution to the flow rate displaced in the medium, recent studies point out that in some cases the temporal evolution of drawdowns in the vicinity of the pumping well displays a power law behavior [e.g., *Bogdanov et al*., 2003; *Le Borgne et al*., 2004; *Chang et al*., 2011]. We contend that the latter is associated with the joint contribution of the fracture and of the rock matrix to the flow rate extracted at the pumping well.

We ground our theoretical analysis on drawdown data collected at the Hydrogeological Experimental Site (HES) in Poitiers, France [*Audouin et al*., 2008; *Riva et al*., 2009; *Trottier et al*., 2014]. To the best of our knowledge, this is the first study providing a theoretically rigorous analysis of the information that can be extracted from reciprocity gaps associated with drawdown signals of the kind observed during interference pumping tests in a fractured system with the aim of providing information about the hydraulic behavior of the fractured-matrix medium, with emphasis on the temporal evolution of drawdowns.

The work is organized as follows. Section 2 motivates the work through a brief illustration of the HES field site which constitutes an example of a karstified domain where interference tests have been performed and both reciprocal and nonreciprocal drawdown curves have been reported. Section 3 presents the mathematical analyses associated with applications of the reciprocity theorem by considering a cross-hole pumping test in a fractured medium; here flow is interpreted through a dual porosity formulation where the pumping well is treated according to diverse modeling alternatives. This framework is then applied in section 4 to the analysis of interference tests performed at the site to illustrate our approach for the characterization of the contribution of the rock matrix to the global flow rate extracted from the fractured medium.

2. Reciprocity Gaps Observed at the HES Site

Reciprocal and nonreciprocal drawdown curves were recorded during the interference tests performed at the Hydrogeological Experimental Site (HES) in Poitiers, France. The site has been extensively characterized

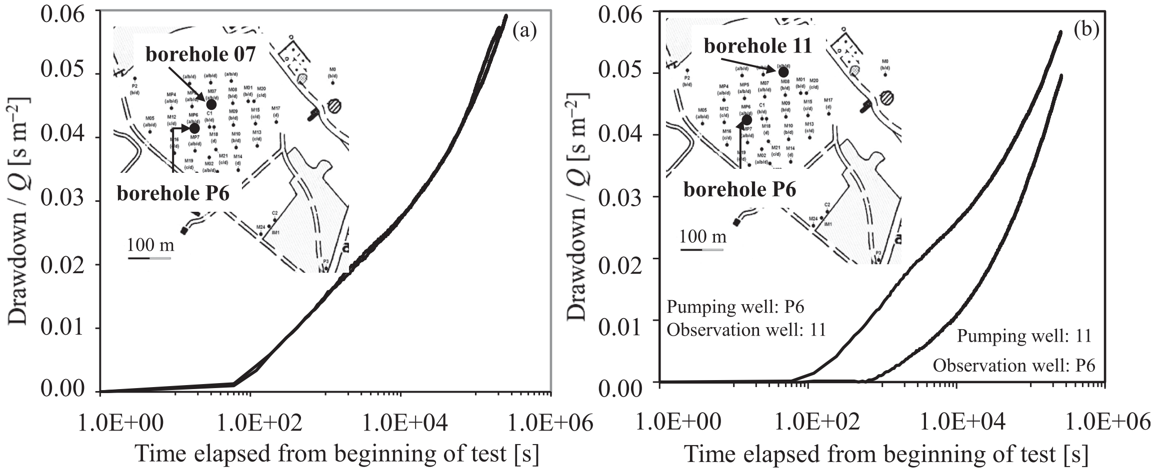

Figure 1. Drawdown curves observed during interference pumping tests performed at the Hydrogeological Experimental Site (HES): (a) example of reciprocity detected between wells P6 and 07; (b) example of observed reciprocity gaps between wells P6 and 11. Figure adapted from *Delay et al*. [2011].

by exploratory analysis, including geophysical, sedimentological, petrophysical, and hydraulic testing, as documented by *Pourpak et al*. [2009] and *De Dreuzy et al*. [2006]. The host geological system is a fractured medium with the presence of open karstic conduits. Seismic data interpretation suggested that the site can be characterized as a three-dimensional complex system where high-porosity bodies are embedded in a low-porosity (compact) matrix, thus supporting a conceptualization of the medium as a dual continuum for the purpose of flow dynamics analyses [e.g., *Kaczmaryk and Delay*, 2007].

Interference tests were performed through a standard procedure according to which water is extracted at a constant flow rate from a well and drawdowns are monitored at all other wells. Pumping was performed sequentially at selected wells within the site, each test lasting 60–120 h of pumping, followed by a relaxation period of a few days to enable heads to return to their initial levels. Additional test operational details are presented by *Kaczmaryk and Delay* [2007] and *Riva et al*. [2009].

An example of observed reciprocal and nonreciprocal drawdowns which can be associated with the same pumping location is depicted in Figure 1. When data from wells P6 and 07 are jointly analyzed, the drawdown curves are starkly reciprocal (Figure 1a). Otherwise, drawdown curves recorded from the interference test performed between wells P6 and 11 (Figure 1b) are nonreciprocal. Viewing the problem through a classical analysis of point-to-point connectivity based on the time elapsed between start of pumping and first response at the observation well [e.g., *Trinchero et al*., 2008; *Fernandez-Garcia et al*., 2010], the observed data would imply that P6 is less connected (in hydraulic terms) to 11 than 11 is to P6 (drawdowns in P6 while pumping in P11 appear later than drawdowns in P11 when pumping in P6; see Figure 1b).

Additional analysis of this observed behavior could be based on the work of *Meier et al*. [1998] and *Sanchez-Vila et al*. [1999]. According to these authors, in a single-continuum representation of the system and after long times, all drawdown curves should display the same slope when viewed in a drawdown versus log-time plot; such slope is directly related to the effective transmissivity of the site. Figure 1b shows that the slope of the drawdown curve recorded when pumping takes place at point 11 displays a late time slope which is higher than that observed when pumping takes place at well P6. On the basis of the results depicted in Figure 1a, the behavior observed in Figure 1b is an additional indication that it is not possible to model the flow response around well 11 as a single continuum.

3. Effect of the Choice of Boundary Conditions at the Pumping Well in a Dual Porosity Model for the Characterization of Reciprocity Gaps

We conceptualize a fractured system by means of a dual porosity model. The system of equations driving flow in such a system is

$$\nabla \cdot \left(K\nabla\psi^f\right)(\boldsymbol{x},t)=S_s^f(\boldsymbol{x})\frac{\partial\psi^f(\boldsymbol{x},t)}{\partial t}+\sigma(\boldsymbol{x})\left(\psi^f(\boldsymbol{x},t)-\psi^m(\boldsymbol{x},t)\right), \quad x\in\Omega, \tag{1}$$

$$S_s^m(\boldsymbol{x})\frac{\partial\psi^m(\boldsymbol{x},t)}{\partial t}=\sigma(\boldsymbol{x})\left(\psi^f(\boldsymbol{x},t)-\psi^m(\boldsymbol{x},t)\right). \quad x\in\Omega. \tag{2}$$

Here superscripts f and m refer to fracture and matrix continua, respectively; $\psi^i(\boldsymbol{x},t)$ (i=f, m) is drawdown [L] at vector location $\boldsymbol{x}$ and time t in the domain Ω, defined as the difference between the initial head and that driven by pumping; $S_s^i(\boldsymbol{x})$ ($i=f$, m) is specific storage [L^{-1}]; $\sigma(\boldsymbol{x})$ [L^{-1} T^{-1}] is a spatially variable parameter controlling the mass of fluid transferred between fracture and matrix, driven by the pressure/head differences locally existing between the two continua; and $\boldsymbol{u}^f(\boldsymbol{x},t)=K(\boldsymbol{x})\nabla\psi^f(\boldsymbol{x},t)$ is the water flux [L T^{-1}], assumed to take place solely in the fractures (notice that from the definition of drawdown, $\nabla\psi(\boldsymbol{x},t)=-\nabla h(\boldsymbol{x},t)$), $K(\boldsymbol{x})$ [L T^{-1}] being hydraulic conductivity of the fracture continuum. Equations (1) and (2) are supplemented by appropriate initial and boundary conditions. Regarding the former, we consider zero initial drawdown at all points, i.e., $\psi^f(\boldsymbol{x},t=0)=\psi^m(\boldsymbol{x},t=0)=0$.

We then assume homogeneous boundary conditions at all points along the external domain boundary. As opposed to *Delay et al*. [2011], we explicitly treat the pumping well as an internal boundary, where the volume of water pumped is given as the sum of the volume extracted directly from the fracture and that supplied from the matrix, i.e.,

$$-\int_{\partial\Omega} K(\boldsymbol{x})\frac{\partial\psi^f}{\partial r}(\boldsymbol{x},t)d\Gamma+\int_{\partial\Omega}\alpha(\boldsymbol{x})\ \left(\psi^f(\boldsymbol{x},t)-\psi^m(\boldsymbol{x},t)\right)d\Gamma=Q_w(t), \tag{3}$$

$Q_w(t)$ and $\partial\Omega$, respectively, being the pumping rate taking place at the well and the surface area of the well boundary; here purely convergent flow is assumed in the close proximity of the well. Note that cylindrical coordinates are implied, i.e., $\boldsymbol{x}=(r,\theta,z)$, in (3) and in all subsequent equations with the origin of coordinates always centered at the selected pumping well. The sign convention adopted implies that Q_w is positive when drawdown is positive (i.e., water is extracted from the well). The quantity $\alpha(\boldsymbol{x})$ [T^{-1}] in (3) deserves some comments. The model considers that the flow rate at the well is supplied by the joint effects of the head (or drawdown) gradient within the fracture continuum and the head/drawdown difference between the two continua (fracture and matrix), $\alpha(\boldsymbol{x})$ being a parameter indicating the potential of the matrix to contribute to the total flow extracted. This contribution is directly related to the local (i.e., at the well location) value of $\sigma(\boldsymbol{x})$, as well as to the radius of the well, r_w. As an example, assuming that σ and drawdown values are uniform along the vertical at the well location, and after some algebra, it can be shown from (3) that $\alpha=\frac{1}{2}\sigma r_w$.

As $\boldsymbol{u}^f(\boldsymbol{x},t)$ is linearly proportional to the drawdown gradient, it is possible to apply Lorentz's principle of reciprocity between ψ^f and the Hermitian operator $\nabla\cdot\nabla$. Casting the problem in Laplace space allows writing the principle of reciprocity as

$$\begin{aligned}&\int_{\Omega}\left(\nabla\cdot\boldsymbol{u}_A^f(\boldsymbol{x},s)\tilde{\psi}_B^f(\boldsymbol{x},s)-\nabla\cdot\boldsymbol{u}_B^f(\boldsymbol{x},s)\tilde{\psi}_A^f(\boldsymbol{x},s)\right)d\Omega=\\&\int_{\partial\Omega}\left(\boldsymbol{u}_B^f(\boldsymbol{x},s)\tilde{\psi}_A^f(\boldsymbol{x},s)-\boldsymbol{u}_A^f(\boldsymbol{x},s)\tilde{\psi}_B^f(\boldsymbol{x},s)\right)\cdot\boldsymbol{n}\ d\Gamma,\end{aligned} \tag{4}$$

where, $\psi_j^f(\boldsymbol{x},t)$ and $\boldsymbol{u}_j^f(\boldsymbol{x},t)$, respectively, are drawdown and flux associated with the fracture continuum when pumping is performed at location $j=A$, B; $\boldsymbol{n}$ is the unit vector normal to the well surface (positive outward); superscript $\sim$ indicates that the corresponding function is expressed in Laplace space, s being the Laplace parameter. It can be shown that the left-hand side of (4) vanishes (see Appendix A). Thus,

$$\int_{\partial\Omega}\tilde{\psi}_A^f(\boldsymbol{x},s)\boldsymbol{u}_B^f(\boldsymbol{x},s)\cdot\boldsymbol{n}\ d\Gamma=\int_{\partial\Omega}\tilde{\psi}_B^f(\boldsymbol{x},s)\boldsymbol{u}_A^f(\boldsymbol{x},s)\cdot\boldsymbol{n}\ d\Gamma. \tag{5}$$

Note that (5) is characterized by one well being active, extracting a flow rate $Q_j(t)$ ($j=A$, B), the other one being inactive. Rewriting (5), introducing the corresponding subscripts in Ω, Γ to denote that the integrals are performed at the well locations (either A or B), yields

$$\int_{\partial\Omega_B} \tilde{\psi}_A^f(\boldsymbol{x},s)K(\boldsymbol{x})\frac{\partial\tilde{\psi}_B^f(\boldsymbol{x},s)}{\partial r}\ d\Gamma_B = \int_{\partial\Omega_A} \tilde{\psi}_B^f(\boldsymbol{x},s)K(\boldsymbol{x})\frac{\partial\tilde{\psi}_A^f(\boldsymbol{x},s)}{\partial r}d\Gamma_A. \tag{6}$$

Finally, introducing the boundary conditions (3) for wells A and B, respectively, pumped at flow rates Q_A and Q_B, assuming that the drawdown in the fracture continuum is uniform along open boreholes at the observation location and that the difference $\left(\psi^f(\boldsymbol{x},t)-\psi^m(\boldsymbol{x},t)\right)$ is relatively uniform along the pumped borehole, leads to

$$\begin{aligned}&\tilde{\psi}_B^f(\boldsymbol{x}_A,s)\left(\tilde{Q}_A(s)-\mu_A\left(\tilde{\psi}_A^f(\boldsymbol{x}_A,s)-\tilde{\psi}_A^m(\boldsymbol{x}_A,s)\right)\right)=\\&\tilde{\psi}_A^f(\boldsymbol{x}_B,s)\left(\tilde{Q}_B(s)-\mu_B\left(\tilde{\psi}_B^f(\boldsymbol{x}_B,s)-\tilde{\psi}_B^m(\boldsymbol{x}_B,s)\right)\right),\end{aligned} \tag{7}$$

where $\mu_j=\int_{\partial\Omega_j}\alpha(\boldsymbol{x})\ d\Gamma$, ($j=A, B$).

As opposed to the results of *Delay et al*. [2011] associated with a single continuum, here we find from (7) that in general $\tilde{Q}_A(s)\tilde{\psi}_B^f(\boldsymbol{x}_A,s) \neq \tilde{Q}_B(s)\tilde{\psi}_A^f(\boldsymbol{x}_B,s)$. Therefore, reciprocity of drawdowns observed in the fractures is not guaranteed with the exception of the special case where $\mu_A=\mu_B=0$, or when the drawdowns in the fracture and matrix coincide at all times, the latter condition being representative of a very fast exchange between the two continua (i.e., the dual continua medium is effectively behaving as a single continuum).

The solution presented in (7) is thus linked to our choice of boundary condition according to which one models the pumping well. A different scheme was investigated by *Delay et al*. [2011], who represent the well as a sink/source term operating in the fracture continuum. By relying on this choice, considering homogeneous initial conditions and casting the problem in Laplace space, *Delay et al*. [2011] found (see their equations (30) and (36b), as well as Appendix A),

$$\begin{aligned}&\tilde{Q}_A(\boldsymbol{x}_A,s)\,\tilde{\psi}_B^f(\boldsymbol{x}_A,s) - \int_\Omega \sigma(\boldsymbol{x})\tilde{\psi}_A^m(\boldsymbol{x},s)\,\tilde{\psi}_B^f(\boldsymbol{x},s)d\Omega \ =\\&\tilde{Q}_B(\boldsymbol{x}_B,s)\,\tilde{\psi}_A^f(\boldsymbol{x}_B,s) - \int_\Omega \sigma(\boldsymbol{x})\tilde{\psi}_B^m(\boldsymbol{x},s)\,\tilde{\psi}_A^f(\boldsymbol{x},s)d\Omega\ .\end{aligned} \tag{8a}$$

$$\tilde{\psi}_j^m(\boldsymbol{x},s) = \frac{\beta(\boldsymbol{x})}{s+\beta(\boldsymbol{x})}\,\tilde{\psi}_j^f(\boldsymbol{x},s)\ , \tag{8b}$$

where $\beta(\boldsymbol{x})=\sigma(\boldsymbol{x})/S_s^m(\boldsymbol{x})$, $\tilde{Q}_j$ being the Laplace transform of the flow rate pumped from the fracture continuum at location $\boldsymbol{x}_j$ ($j=A, B$). Substitution of (8b) in (8a) yields $\tilde{Q}_A(\boldsymbol{x}_A,s)\,\tilde{\psi}_B^f(\boldsymbol{x}_A,s)=\tilde{Q}_B(\boldsymbol{x}_B,s)\,\tilde{\psi}_A^f(\boldsymbol{x}_B,s)$ so that reciprocity of drawdowns in the fracture continuum holds when withdrawal histories at A and B are proportional, i.e., $Q_A(\boldsymbol{x}_A,t)=c\,Q_B(\boldsymbol{x}_B,t)$, c being a constant.

Comparison of (7) and (8) suggests that in a dual porosity model treating the well either as a source/sink term in the fracture or as a boundary condition (in the way we do in (3)) leads to diverse interpretations of conditions of occurrence of reciprocity gaps as well as to diverse quantifications of the temporal dynamics of such gaps, as driven by the conceptual model employed for the representation of the medium.

4. Characterization of Rock Matrix Contribution to Total Extracted Flow Rate

Here we explore the application of (7) to provide information about the way the rock matrix contributes to the global flow rate conveyed through the medium in the modeling context analyzed. We start by noting that in interference tests, the observables are the flow rate and drawdowns at the pumping and observation boreholes [e.g., *Illman*, 2014 and references therein]. We employ here the common assumption [e.g., *Bourbiaux*, 2010] that a measurement device (e.g., a pressure transducer) placed at a borehole provides information mostly about the drawdown at the fracture. As such, corresponding drawdowns in the matrix cannot be properly measured in general and might only be inferred indirectly.

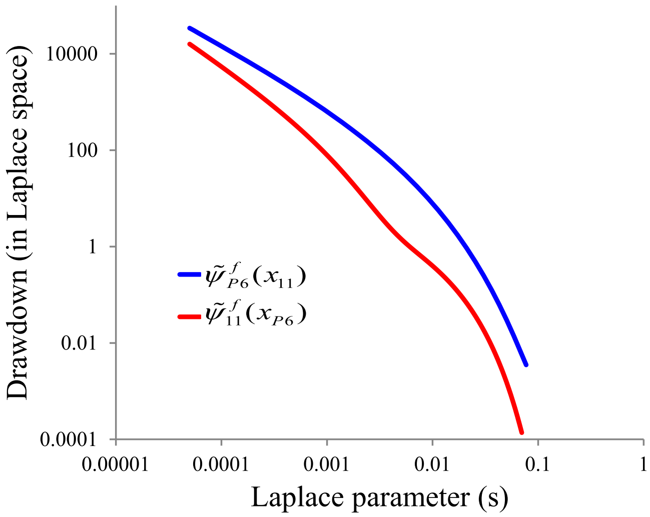

Figure 2. Discrete Laplace transform of the drawdown data observed at well 11 when pumping is performed at well P6 (in blue) and of drawdowns measured at P6 when pumping in 11 (in red). Curves are constructed by transforming the drawdown data depicted in Figure 1b to Laplace space.

Thus, in a classical interference test between locations A and B, measurements of $\tilde{Q}_A(s)$, $\tilde{Q}_B(s)$, $\tilde{\psi}^f_A(\boldsymbol{x}_A,s)$, $\tilde{\psi}^f_B(\boldsymbol{x}_A,s)$, $\tilde{\psi}^f_A(\boldsymbol{x}_B,s)$, and $\tilde{\psi}^f_B(\boldsymbol{x}_B,s)$ are typically available. The coefficients μ_A, μ_B in (7) and the functions $\tilde{\psi}^m_A(\boldsymbol{x}_A,s)$, $\tilde{\psi}^m_B(\boldsymbol{x}_B,s)$, representing drawdowns in the matrix at locations where pumping takes place, are typically unknown. Each additional pumping/observation point included would result in an additional set of unknown quantities, which are given by the corresponding values of μ and $\tilde{\psi}^m$. On these bases, we explore, through observations from the field scale interference pumping test illustrated in section 2, the way the analysis of detected reciprocity gaps can lead to characterizing the contribution of the matrix to the flow rate extracted at the well.

We recall here Figure 1a, i.e., the drawdown curves recorded at wells P6 and 07 during the interference test. In this case, the drawdown curves display a clear reciprocal behavior. When this observation is implemented in (7), it is concluded that

$$\mu_j\left(\tilde{\psi}^f_j(\boldsymbol{x}_j,s)-\tilde{\psi}^m_j(\boldsymbol{x}_j,s)\right) = 0, \quad (j=\text{ P6, 07}). \tag{9}$$

We note that emergence of reciprocity does not necessarily imply that the system should be interpreted as a single continuum. In the context of a dual porosity formulation, it could imply that the flow extracted at the well location is supplied by the fractures in the system, with zero or very limited contribution from the matrix (see (8) and associated discussion). However, a nonreciprocal behavior was observed for the drawdowns recorded in the interference test performed between wells P6 and 11 (Figure 1b).

To interpret the nonreciprocal drawdown curves in Figure 1b, we start by combining (7) and (9), to obtain

$$\frac{\tilde{\psi}^f_{11}(\boldsymbol{x}_{P6},s)}{\tilde{Q}_{11}(s)}=\frac{\tilde{\psi}^f_{P6}(\boldsymbol{x}_{11},s)}{\tilde{Q}_{P6}(s)}\left[1-\frac{1}{\tilde{Q}_{11}(s)}\mu_{11}\left(\tilde{\psi}^f_{11}(\boldsymbol{x}_{11},s)-\tilde{\psi}^m_{11}(\boldsymbol{x}_{11},s)\right)\right], \tag{10}$$

where the subscripts for drawdowns $\tilde{\psi}$ and parameters μ and Q refer to the pumped well, while those for $\boldsymbol{x}$ denote location where the observation took place (either pumping or observation points).

Equation (10) should enable us to estimate μ_{11} and $\tilde{\psi}^m_{11}(\boldsymbol{x}_{11},s)$ if all remaining quantities were available. Drawdowns measured at the pumping wells could not be used at HES, as head losses could not be filtered from the signal at the pumping location, as it is common in most practical applications. As a consequence, the joint use of (10) and available data allows estimating solely the product $\mu_{11}\left(\tilde{\psi}^f_{11}(\boldsymbol{x}_{11},s)-\tilde{\psi}^m_{11}(\boldsymbol{x}_{11},s)\right)$.

Both tests were performed with constant pumping rates, $Q_j(t)=Q_j\,H(t)$ ($Q_j=62.8$ or 59.0 m^3 h^{-1}, respectively, for $j=$ P6 or 11), $H(t)$ being the Heaviside function. The corresponding Laplace transform is $\tilde{Q}_j(s)\ =\tilde{Q}_j(s)=Q_j/s$. Applying Laplace transform to the drawdown data, and assuming these represent those of the fractures, we can then get $\tilde{\psi}^f_{11}(\boldsymbol{x}_{P6},s)$ and $\tilde{\psi}^f_{P6}(\boldsymbol{x}_{11},s)$, as depicted in Figure 2. Figure 3 depicts the function $\mu_{11}\left(\tilde{\psi}^f_{11}(\boldsymbol{x}_{11},s)-\tilde{\psi}^m_{11}(\boldsymbol{x}_{11},s)\right)$, as calculated from (10). A regression line obtained as best fit of the data for low s values (corresponding to long times) is also depicted. From Figure 3, and noticing that μ_{11} is a constant, one obtains

$$\left(\tilde{\psi}^f_{11}(\boldsymbol{x}_{11},s)-\tilde{\psi}^m_{11}(\boldsymbol{x}_{11},s)\right)\sim s^{-\beta}, \tag{11}$$

associated with an estimate of $\beta=0.82$ (obtained on the basis of visual inspection). As a consequence, the

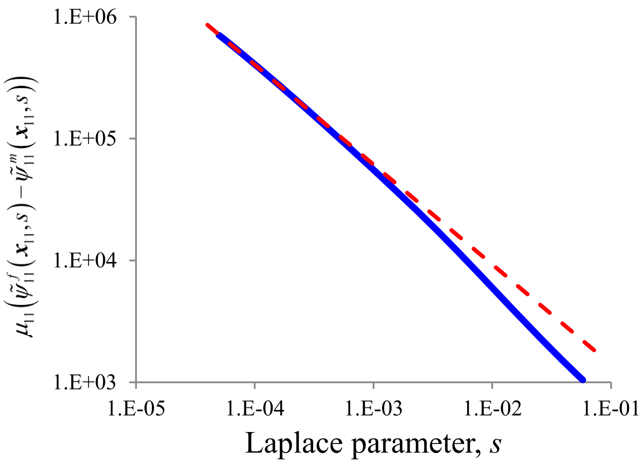

Figure 3. Blue (solid) curve: estimate of the fracture-matrix drawdown differential, $\mu_{11}\left(\tilde{\psi}^{f}_{11}(\boldsymbol{x}_{11},s)-\tilde{\psi}^{m}_{11}(\boldsymbol{x}_{11},s)\right)$, based on the data from the test depicted in Figure 2 and (9); red (dashed) line: best linear estimate (in log-log space) obtained using only data for small values of the Laplace parameter s, indicating a power law behavior.

difference between drawdowns observed within the fracture and matrix continua at the pumping well in real space displays a power law behavior,

$$\left(\tilde{\psi}^{f}_{11}(\boldsymbol{x}_{11},t)-\tilde{\psi}^{m}_{11}(\boldsymbol{x}_{11},t)\right)\sim t^{(\beta-1)}, \tag{12}$$

where the exponent in the power law results in $t^{-0.18}$ indicating that the difference tends to vanish for (very) long times. The asymptotic behavior we document suggests that reciprocity gaps associated with an interpretation based on a dual porosity model upon treating the pumping well as a boundary condition tend to disappear for long pumping times, in agreement with the conceptual picture presented by *Acuna et al.* [1995], *Acuna and Yortsos* [1995], and *Delay et al.* [2011]. Yet these gaps remain for very long times in practical applications of the kind we analyzed here.

As discussed in section 3, reciprocity in the fracture drawdowns takes place whenever water is only extracted from the fracture, even as a dual continuum conceptual model is invoked to depict the system behavior, provided that $Q_A(\boldsymbol{x}_A,t)=c\,Q_B(\boldsymbol{x}_B,t)$. Here we showed that whenever it is considered that the matrix partially contributes to the total flow rate extracted, nonreciprocity is expected, as linked to the occurrence of a differential drawdown between fracture and matrix. This difference decreases with time in the example presented, displaying a power law late time behavior, characterized by a small (negative) exponent.

5. Conclusions

Our work leads to the following major conclusions:

1. We show that interpreting a fractured medium as a dual porosity continuum can cause reciprocal and nonreciprocal behavior of drawdown in modeled interference tests to coexist in a given area, as these are related to the local ability of the matrix to contribute to the total flow extracted at the pumping well.
2. We demonstrate that the way the pumping well is treated in a dual porosity model (i.e., as a source/sink term acting in the fracture or as a prescribed flow rate boundary, where the contribution of the matrix to the extracted flow rate is included) has a significant impact on the way reciprocity gaps can emerge and be quantified in the fracture continuum. In this modeling context, absence of drawdown reciprocity gaps might suggest that water is extracted from the fractures, with no contribution from the matrix. That is, the occurrence of reciprocal drawdowns does not necessarily imply that the system behaves as a single continuum so that a dual continuum conceptualization can still form the basis for the description of the flow features in a fractured host formation.
3. We explore and quantify for the first time the asymptotic (for long observation times) behavior at the pumping well of the difference between drawdowns associated with the fracture and matrix continua in a dual porosity representation of fractured geological media subject to interference hydraulic tests. Our theoretical results are employed to identify the matrix contribution to the flow being supplied to the pumping well by the host rock formation. This identification is based on actual data from an interference test performed at a fissured confined karstic formation (HES Site, France). We show that whenever the matrix is assumed to provide a contribution to the total flow rate extracted (a) the resulting nonreciprocity of drawdowns can be employed to quantify such contribution, and (b) the difference between the

drawdowns in the fracture and rock continua at the well tends to decrease by following a power law late time behavior, with nonreciprocity effect persisting up to very long times.

Appendix A

The starting point is the coupled system of partial differential equations given in (1) and (2). Rewriting these equations in Laplace space leads to

$$\nabla \cdot \boldsymbol{u}^f(\boldsymbol{x},s) = sS_s^f(\boldsymbol{x})\tilde{\psi}^f(\boldsymbol{x},s) + \sigma(\boldsymbol{x})\left(\tilde{\psi}^f(\boldsymbol{x},s) - \tilde{\psi}^m(\boldsymbol{x},s)\right), \tag{A1}$$

$$sS_s^m(\boldsymbol{x})\tilde{\psi}^m(\boldsymbol{x},s) = \sigma(\boldsymbol{x})\left(\tilde{\psi}^f(\boldsymbol{x},s) - \tilde{\psi}^m(\boldsymbol{x},s)\right). \tag{A2}$$

From (A2), we obtain

$$\tilde{\psi}^m(\boldsymbol{x},s) = \frac{\beta(\boldsymbol{x})}{s+\beta(\boldsymbol{x})}\tilde{\psi}^f(\boldsymbol{x},s), \tag{A3}$$

where $\beta(\boldsymbol{x}) = \sigma(\boldsymbol{x})/S_s^m(\boldsymbol{x})$. Replacing (A3) into (A1) leads to

$$\nabla \cdot \boldsymbol{u}^f(\boldsymbol{x},s) = sS_s^f(\boldsymbol{x})\tilde{\psi}^f(\boldsymbol{x},s) + \frac{s\sigma(\boldsymbol{x})}{s+\beta(\boldsymbol{x})}\tilde{\psi}^f(\boldsymbol{x},s). \tag{A4}$$

One can then evaluate the left-hand side of (5) through the use of (A4)

$$\int_\Omega \left(\nabla \cdot \boldsymbol{u}_A^f(\boldsymbol{x},s)\tilde{\psi}_B^f(\boldsymbol{x},s) - \nabla \cdot \boldsymbol{u}_B^f(\boldsymbol{x},s)\tilde{\psi}_A^f(\boldsymbol{x},s)\right) d\Omega =$$
$$\int_\Omega \left[\begin{array}{l} \left(sS_s^f(\boldsymbol{x})\tilde{\psi}_A^f(\boldsymbol{x},s) + \dfrac{s\sigma(\boldsymbol{x})}{s+\beta(\boldsymbol{x})}\tilde{\psi}_A^f(\boldsymbol{x},s)\right)\tilde{\psi}_B^f(\boldsymbol{x},s) \\ -\left(sS_s^f(\boldsymbol{x})\tilde{\psi}_B^f(\boldsymbol{x},s) + \dfrac{s\sigma(\boldsymbol{x})}{s+\beta(\boldsymbol{x})}\tilde{\psi}_B^f(\boldsymbol{x},s)\right)\tilde{\psi}_A^f(\boldsymbol{x},s) \end{array}\right] d\Omega \;=\; 0. \tag{A5}$$

Acknowledgments
A.G. acknowledges funding from MIUR (Ministry of Education, Universities and Research (Italy) - PRIN2010-11; project: "Innovative methods for water resources under hydro-climatic uncertainty scenarios"). X.S. acknowledges funding from the ICREA Academia Program and from the EU 7th Framework Programme for Research, Technological Development and Demonstration, grant agreement 619120 (project MARSOL). The authors commit to make their data available and refer the reader to the corresponding author.

References

Acuna, J. A., and Y. C. Yortsos (1995), Application of fractal geometry to the study of networks of fractures and their pressure transient, *Water Resour. Res.*, *31*(3), 527–540.

Acuna, J. A., I. Ershaghi, and Y. C. Yortsos (1995), Practical applications of fractal pressure transient analysis of naturally fractured reservoirs, *SPE Form. Eval.*, *10*, 173–179.

Audouin, O., J. Bodin, G. Porel, and B. Bourbiaux (2008), Flowpath structure in a limestone aquifer: Multi-borehole logging investigations at the hydrogeological experimental site of Poitiers, France, *Hydrogeol. J.*, *16*(5), 939–950.

Bailly, D., R. Ababou, and M. Quintard (2009), Geometric characterization, hydraulic behavior and upscaling of 3-D fissured geologic media, *Math. Comput. Simul.*, *79*, 3385–3396.

Berkowitz, B. (2002), Characterizing flow and transport in fractured geological media: A review, *Adv. Water Resour.*, *25*, 861–884.

Bogdanov, I. I., V. V. Mourzenko, J.-F. Thovert, and P. M. Adler (2003), Pressure drawdown well tests in fractured porous media, *Water Resour. Res.*, *39*(1), 1021, doi:10.1029/2000WR000080.

Bourbiaux, B. (2010), Fractured reservoir simulations: A challenging and rewarding issue, *Oil Gas Sci. Technol.*, *65*(2), 227–238, doi:10.2516/ogst/2009063.

Bruggeman, G. A. (1972), The reciprocity principle in flow through heterogeneous porous media, in *Fundamentals of Transport in Porous Media*, pp. 135–149, Elsevier, Amsterdam.

Chang, Y.-C., H.-D. Yeh, K.-F. Liang, and M.-C.T. Kuo (2011), Scale dependency of fractional flow dimension in a fractured formation, *Hydrol. Earth Syst. Sci.*, *15*, 2165–2178, doi:10.5194/hess-15-2165-2011.

De Dreuzy, J. R., J. Bodin, H. Le Grand, P. Davy, D. Boulanger, A. Battais, O. Bour, P. Gouze, and G. Porel (2006), General database for ground water site information, *Ground Water*, *44*(5), 743–748.

Delay, F., P. Ackerer, and A. Guadagnini (2011), Theoretical analysis and field evidence of reciprocity gaps during interference pumping tests, *Adv. Water Resour.*, *34*(5), 592–606, doi:10.1016/j.advwatres.2011.02.006.

Delay, F., P. Ackerer, B. Belfort, and A. Guadagnini (2012), On the emergence of reciprocity gaps during interference pumping tests in unconfined aquifers, *Adv. Water Resour.*, *46*, 11–19, doi:10.1016/j.advwatres.2012.06.002.

Dershowitz, W., and I. Miller (1995), Dual porosity fracture flow and transport, *Geophys. Res. Lett.*, *22*(11), 1441–1444.

De Smedt, M. (2011), Analytical solution for constant-rate pumping test in fissured porous media with Double-Porosity behaviour, *Transp. Porous Media*, *88*, 479–489, doi:10.1007/s11242-011-9750-9.

Fernandez-Garcia, D., P. Trinchero, and X. Sanchez-Vila (2010), Conditional stochastic mapping of transport connectivity, *Water Resour. Res.*, *46*, W10515, doi:10.1029/2009WR008533.

Ghasemizadeh, R., F. Hellweger, C. Butscher, I. Padilla, D. Vesper, M. Field, and A. Alshawabkeh (2012), Review: Groundwater flow and transport modeling of karst aquifers, with particular reference to the North Coast Limestone aquifer system of Puerto Rico, *Hydrogeol. J.*, *20*(8), 1441–1461, doi:10.1007/s10040-012-0897-4.

Huang, W., G. Di Donato, and M. J. Blunt (2004), Comparison of streamline-based and grid-based dual porosity simulations, *SPE J.*, *43*(2), 129–137.

Huyakorn, P. S., B. H. Lester, and C. R. Faust (1983), Finite element technique for modeling groundwater flow in fractured aquifers, *Water Resour. Res.*, *19*(4), 1019–1035.

Illman, W. A. (2014), Hydraulic tomography offers improved imaging of heterogeneity in fractured rocks, *Ground Water*, *52*(5), 659–684, doi:10.1111/gwat.12119.

Kaczmaryk, A., and F. Delay (2007), Interpretation of interference pumping test in fractured limestone by means of dual-medium approaches, *J. Hydrol.*, *337*, 133–146, doi:10.1016/j.jhydrol.2007.01.004.

Le Borgne, T., J. R. De Dreuzy, P. Davy, and F. Touchard (2004), Equivalent mean flow models for fractured aquifers: Insights from a pumping tests scaling interpretation, *Water Resour. Res.*, *40*, W03512, doi:10.1029/2003WR002436.

Mao, D., T.-C. J. Yeh, L. Wan, C.-H. Lee, K.-C. Hsu, J.-C. Wen, and W. Lu (2013), Cross-correlation analysis and information content of observed heads during pumping in unconfined aquifers, *Water Resour. Res.*, *49*, 713–731, doi:10.1002/wrcr.20066.

Maréchal, J.-C., B. Ladouche, N. Dörfliger, and P. Lachassagne (2008), Interpretation of pumping tests in a mixed flow karst system, *Water Resour. Res.*, *44*, W05401, doi:10.1029/2007WR006288.

Meier, P. M., J. Carrera, and X. Sanchez-Vila (1998), An evaluation of Jacob's method for the interpretation of pumping tests in heterogeneous formations, *Water Resour. Res.*, *34*(5), 1011–1025, doi:10.1029/98WR00008.

Neuman, S. P. (2005), Trends, prospects and challenges in quantifying flow and transport through fractured rocks, *Hydrogeol. J.*, *13*, 124–147.

Pourpak, H., B. Bourbiaux, F. Roggero, and F. Delay (2009), An integrated methodo-logy for calibrating a heterogeneous fractured reservoir model from wellbore flow measurements: Case study, *SPE J.*, *12*, 433–445.

Raghavan, R. (2009), Complex geology and pressure tests, *J. Pet. Sci. Eng.*, *69*, 181–188.

Riva, M., A. Guadagnini, J. Bodin, and F. Delay (2009), Characterization of the Hydrogeological Site of Poitiers–France by stochastic well testing analysis, *J. Hydrol.*, *369*, 154–164, doi:10.1016/j.jhydrol.2009.02.040.

Sahimi, M. (2011), *Flow and Transport in Porous Media and Fractured Rocks*, 709 pp., John Wiley, Hoboken, N. J.

Samardzioska, T., and V. Popov (2005), Numerical comparison of the equivalent continuum, non-homogeneous and dual porosity models for flow and transport in fractured porous media, *Adv. Water Resour.*, *28*, 235–255.

Sanchez-Vila, X., P. M. Meier, and J. Carrera (1999), Pumping tests in heterogeneous aquifers: An analytical study of what can be obtained from their interpretation using Jacob's method, *Water Resour. Res.*, *35*(4), 943–952, doi:10.1029/1999WR900007.

Trinchero, P., X. Sanchez-Vila, and D. Fernandez-Garcia (2008), Point-to-point connectivity, an abstract concept or a key issue for risk assessment studies?, *Adv. Water Res.*, *31*(12), 1742–1753, doi:10.1016/j.advwatres.2008.09.001.

Trottier, N., F. Delay, O. Bildstein, and P. Ackerer (2014), Inversion of a dual-continuum approach to flow in a karstified limestone: Insight into heterogeneity revealed by well-test interferences, *J. Hydrol.*, *508*, 157–169.